Time-dependent electron phenomena at surfaces

R. Díez Muiño[a,b], D. Sánchez-Portal[a,b], V. M. Silkin[b,c,d], E. V. Chulkov[a,b,c], and P. M. Echenique[a,b,c,1]

[a]Centro de Física de Materiales (CFM-MPC), Consejo Superior de Investigaciones Científicas (CSIC)–Universidad del Pais Vasco (UPV-EHU), Paseo Manuel de Lardizabal 5, 20018 San Sebastián, Spain; [b]Donostia International Physics Center (DIPC), Paseo Manuel de Lardizabal 4, 20018 San Sebastián, Spain; [c]Departamento de Física de Materials, Facultad de Ciencias Químicas, Universidad del Pais Vasco (UPV-EHU), Apartado 1072, 20080 San Sebastián, Spain; and [d]Ikerbasque, Basque Foundation for Science, E-48011 Bilbao, Spain

Edited by John T. Yates, University of Virginia, Charlottesville, VA, and approved October 26, 2010 (received for review June 15, 2010)

Femtosecond and subfemtosecond time scales typically rule electron dynamics at metal surfaces. Recent advance in experimental techniques permits now remarkable precision in the description of these processes. In particular, shorter time scales, smaller system sizes, and spin-dependent effects are current targets of interest. In this article, we use state-of-the-art theoretical methods to analyze these refined features of electron dynamics. We show that the screening of localized charges at metal surfaces is created locally in the attosecond time scale, while collective excitations transfer the perturbation to larger distances in longer time scales. We predict that the elastic width of the resonance in excited alkali adsorbates on ferromagnetic surfaces can depend on spin orientation in a counterintuitive way. Finally, we quantitatively evaluate the electron–electron and electron–phonon contributions to the electronic excited states widths in ultrathin metal layers. We conclude that confinement and spin effects are key factors in the behavior of electron dynamics at metal surfaces.

lifetimes | spin effects | time-dependent phenomena

Chemistry is driven by electrons. Chemical dynamics is often determined by electron dynamics, with electronically excited states frequently acting as necessary intermediate steps in chemical activity. The understanding and control of charge transfer times and electronic excitation survival times is thus a necessary step to understand, control, and design physical and chemical processes at surfaces.

Dynamics of electronic excitations at metal surfaces has been widely investigated both experimentally (1–6) and theoretically (5, 7–13). As a consequence, deep understanding has been reached about the mechanisms ruling electron decay and electron charge transfer. However, recent advances in experimental tools are raising new challenges, many of them linked to shorter time scales, smaller system sizes, and/or spin effects. In this article, we present fresh results on these expanding topics, in an effort to blaze trails in electron dynamics research.

At surfaces, electron excitation, charge exchange, and electron decay typically take place in the femtosecond (fs) and attosecond (as) time scales ($1\ \text{as} = 10^{-18}$ s, $1\ \text{fs} = 10^{-15}$ s) (i.e., at times much faster than any nuclear motion). Advance in laser-based experimental techniques has carried research on this field to a new frontier, in which direct measurements of electron processes in this time scale are possible. Attosecond spectroscopy, for instance, is nowadays able to discern the individual elementary steps in photoemission from surfaces (i.e., excitation, transport, and emission) (14, 15). Access to experimental information in the attosecond scale is asking for new theoretical concepts. In particular, one of the relevant questions is how electronic excitations are created in time and how the environment reacts in such time scale. In the photocreation of localized holes in adsorbates at metallic surfaces, this question can be reformulated as how and when electron screening is built in the subfemtosecond scale. We address this point in the first section of this article.

Ultrafast spin-dependent electron dynamics is another key concept for applied research. Active manipulation and control of magnetic ordering down to a single atomic magnet, such as a single atomic spin on a surface, is of great importance for potential applications in spintronics. The dependence on spin orientation of the lifetime of electronic excitations has been accurately characterized in ferromagnetic bulk (16). How to characterize and tune the spin-polarized transfer of electrons from an adsorbate into the surface remains, however, an open question. Atom/surface combinations for which electron charge transfer times are very much dependent on the spin of the excited electron would make spin-polarized electron transfer controllable at the atomic scale. In the second section of the article, we show that this is actually the case with an example: the spin-selective transfer of electrons from Cs adsorbates into a Fe(110) surface. Previous research on alkali atom adsorption on metal surfaces provided unprecedented understanding of electronic and dynamical properties of these systems (17–22). Nuclear dynamics initiated by the photoexcitation of chemisorbed alkali atoms (19), for instance, can be considered as a remarkable example of standard surface photochemistry. We show that alkali atoms on ferromagnetic surfaces can potentially become a remarkable example of spin photochemistry as well.

From the perspective of size, the possibility of designing, fabricating, and characterizing systems in the nanoscale paves the way for the modulation of electronic excitation lifetimes. However, the dynamics of electronic excitations in finite-size systems is still not fully apprehended. There are several effects that mark a clear difference between the dynamics of hot electrons in metallic bulk and nanosystems. The electron lifetime can be enhanced in confined systems as compared to bulk because of the discretization of levels that reduces the number of final states to which the electronic excitation can decay. The electron lifetime can be shortened in the nanosystem because of the reduction of dynamic screening for low frequencies. Finally, the electron lifetime also can be shortened in the nanosystem because of the quenching of dynamic screening at the surface regions. All in all, there are no simple arguments to predict whether the lifetime of electronic excitations in confined systems is longer or shorter than in bulk.

In the third section of the article, we illustrate the complexity of this problem by showing how dimensionality effects can lead to significant modifications in electronic decay in ultrathin metal films. Strong oscillations in the electron–electron and electron–phonon contributions to the lifetime as a function of the film thickness are found.

We present our conclusions in the last section. Discussion on some future directions in which we expect the field to evolve in the next few years is included as well.

Atomic units (a.u.) are used throughout unless otherwise stated.

Author contributions: P.M.E. designed research; R.D.M., D.S.-P., V.M.S., and E.V.C. performed research; and R.D.M., D.S.-P., V.M.S., E.V.C., and P.M.E. wrote the paper.

The authors declare no conflict of interest.

This article is a PNAS Direct Submission.

[1]To whom correspondence should be addressed. E-mail pedromiguel.echenique@sc.ehu.es.

Time Scale of Localized Hole Screening at Surfaces

Screening is a complex many-body process that substantially reduces the effective interaction range of the positive charge left behind after photoemission of an electron. Screening requires rearrangement of the electronic density in the vicinity of the hole. In semiconductors, the low density of carriers leads to a relatively slow response to an external charge (of the order of a few hundred femtoseconds), and the evolution of the screening process can be directly monitored in time (23). Quantum kinetic theory (24) can describe the nonequilibrium dynamics of the Coulomb interaction in this time scale. In metals, however, the rearrangement of electronic charge making the screening takes place in shorter times—namely, in the attosecond scale. For low kinetic energies of the photoemitted electron, this time scale can be similar to the one required for the electron to leave the surface. Both processes are thus entangled. For high kinetic energies, the photoemitted electron is already far from the surface before the hole screening is built up: The two processes can then be considered as roughly independent. In order to obtain further insight into such a situation, a more precise knowledge of the screening time at metal surfaces is required. This is what we address here, restricting ourselves to a simplified case, that of the screening of a bare positive charge suddenly created in front of a metal surface.

So far, existing theoretical studies of time-dependent Coulomb screening have used a free electron jellium-like description to describe metallic media, either in first-order perturbation theory (25) or in nonperturbative treatments (26). Dimensionality effects in the screening have been addressed as well (27, 28). These works showed that, in a medium in which the electrons are free to move, the screening of a suddenly created charge is built locally in the subfemtosecond scale. At the very first steps of the screening process, a universal scaling law ($\propto 1/r_s^2$) rules the time evolution of the system. Here r_s is the electron density parameter that depends on the electron density n_e through $1/n_e = 4\pi r_s^3/3$. For longer times, the key magnitude is the plasma frequency ω_p, and a different scaling time $1/\omega_p$ is found (26). These longer-time oscillations are relevant for the preasymptotic decay and dephasing of quasiparticles for some surface and image potential states (29).

However, the role of the surface band structure in the establishment of local screening has not been addressed yet. In particular, numerous metal surfaces contain surface electronic states with wave functions strongly localized at the surface. These surface states can often form a sort of 2D electron gas system. In addition to the well-known surface plasmons, new collective electronic excitations, known as acoustic surface plasmons, can arise (30, 31). In these metal surfaces, carriers residing in two electron systems (the 2D surface state and the 3D bulk states) do conjointly participate in the screening process. A well-known example of surfaces in which the 2D and 3D electronic systems coexist is the (111) surface of noble metals like Cu, Ag, and Au, with a partially occupied electron band of the s-p_z surface state at the surface Brillouin zone (BZ) center $\overline{\Gamma}$. These states are frequently considered as forming the quasi 2D surface-state band with the Fermi energy E_F^{SS} equal to the surface-state binding energy at the $\overline{\Gamma}$ point.

In the following, we analyze how the joint response of these two electronic systems of different dimensionality affects the short-time dynamics of screening. We consider a single positive charge e suddenly created near a metal surface. We perform calculations within the framework of linear response theory. Linear response theory underestimates the induced charge density in the close vicinity of the charge but reproduces quite well the time scale of the screening process as well as the induced electronic charge at longer distances (25–28).

The charge e is placed at time $t = 0$ at a position $\mathbf{r}_o = (0,0,z_o)$ in front of a Cu(111) surface. In linear response theory, the electronic charge $n_{ind}(\mathbf{r},\omega)$ induced by such Coulomb potential is:

$$n_{ind}(R,z,\omega) = \frac{1}{2\pi}\int_0^\infty dq_\parallel q_\parallel J_0(q_\parallel R) n_{ind}(q_\parallel,z,\omega) \quad [1]$$

with

$$n_{ind}(q_\parallel,z,\omega) = \int dz' \chi(q_\parallel,z,z',\omega)\frac{2\pi}{q_\parallel} e^{-q_\parallel|z'-z_o|}, \quad [2]$$

where $\mathbf{r} = \{R,z\}$. R is a cylindrical coordinate in the plane parallel to the surface, measured from an axis that goes through the charge. The coordinate z is that normal to the surface. J_0 is the zeroth Bessel function and $q_\parallel$ is the modulus of the 2D momentum $\mathbf{q}_\parallel$ in the plane parallel to the surface. The function χ is the density response function of the Cu(111) surface.

The Cu(111) surface is modeled using a 21-layer slab. We calculate χ numerically in the random phase approximation. Our procedure is similar to that of ref. 30 and is only briefly summarized here. One-electron states necessary to build the noninteracting response χ_0, a previous step in the calculation of χ, are obtained from the solution of a 1D Schrödinger equation for an adequate Cu(111) effective potential (32).

In order to facilitate the discussion on the complex electron excitation spectrum of the Cu(111) surface, we define the surface loss function $g(q_\parallel,\omega)$ as:

$$g(q_\parallel,\omega) = -\frac{2\pi}{q_\parallel}\int dz \int dz' e^{-q_\parallel(z+z')}\chi(q_\parallel,z,z',\omega). \quad [3]$$

The imaginary part of the function $g(q_\parallel,\omega)$ contains information on the rate at which a frequency-dependent external potential generates electron-hole and collective electronic excitations at surfaces. In Fig. 1, we show a normalized 2D plot of $\mathrm{Im}g(q_\parallel,\omega)$ as a function of $q_\parallel$ and ω. A dominant peak ω_{SP} appears, corresponding to the conventional surface plasmon in the 8–12 eV energy range. For $q_\parallel < 0.03$ a.u., this peak splits into two separate ones, corresponding to the symmetrical ω_{SP}^- and antisymmetrical ω_{SP}^+ modes. This is a well-known effect for a finite thickness slab (33). An involved structure is conspicuous in the low energy range of the spectrum. For momenta $q_\parallel > 0.07$ a.u., there are intraband electron-hole transitions within the surface-state bands (34). For smaller momenta, the acoustic surface plasmon ω_{ASP} (30) is clearly seen.

In Fig. 2, we show 2D plots of the induced electronic density $R \times n_{ind}(R,z,t)$ for different values of the time variable t, when the charge e is created at $t = 0$ at a distance $Z = 1.97$ a.u. from the topmost Cu atomic layer. [This distance corresponds to the distance between atomic planes along the (111) direction.] Fig. 2

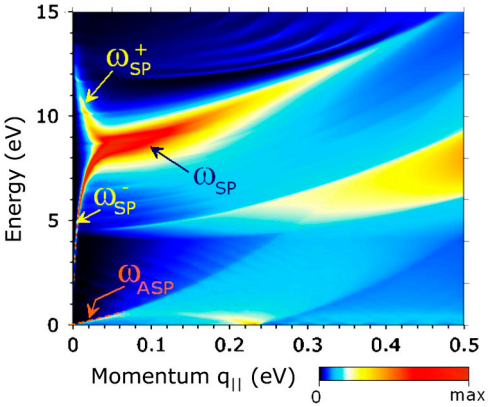

Fig. 1. Two-dimensional plot of the normalized surface loss function $\mathrm{Im}[g(q_\parallel,\omega)]/\omega$ for the 21 ML Cu(111) slab versus the 2D momentum $q_\parallel$ and energy ω. Peaks corresponding to the dominating surface plasmon ω_{SP}, to its split symmetrical ω_{SP}^- and antisymmetrical ω_{SP}^+ modes at small $q_\parallel$s, and to the acoustic surface plasmon ω_{ASP} are denoted by the corresponding symbols.

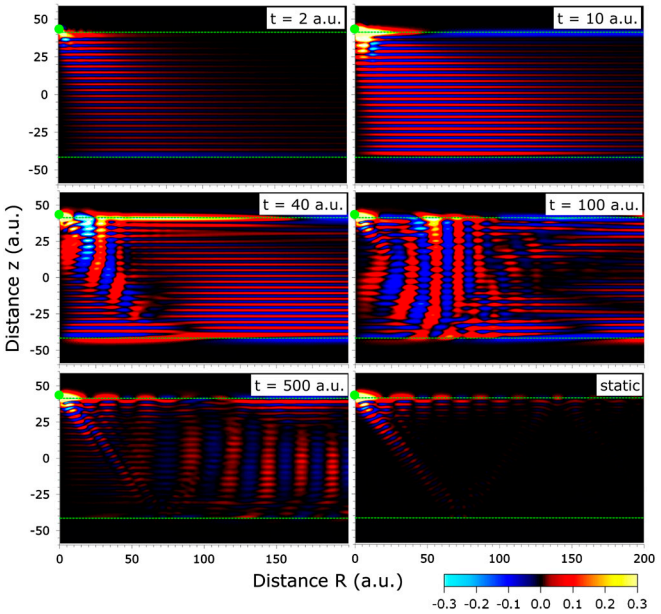

Fig. 2. Interpolated plot of the normalized induced charge density $R \times n_{ind}(R,z,t)$ established in the slab at times $t = 2$, 10, 40, 100, and 500 a.u. when an external point charge is created at time $t = 0$ at a metal surface. The infinite time limit (static case) is shown as well. The charge position is marked by a green filled circle. The density is shown as a function of the lateral distance R from the external charge and the perpendicular coordinate z. Dashed green horizontal lines delimit the slab used in the calculations.

clearly shows that the screening hole around the charge is fully developed within a few a.u. (i.e., in the attosecond time scale; 1 a.u. = 24.2 as). In this initial regime, the electron density rearrangement is not able to resolve the finite size of the slab, and the screening process in the vicinity of the charge is representative of the semiinfinite system. A shock wave forms and propagates in both perpendicular and lateral directions, due to electron-hole pair excitations. This is similar to the propagation in bulk systems. During this initial regime, the electronic propagation is quite isotropic. Strong effects reflecting the band structure of the system (and, in particular, the projected band gap around $\overline{\Gamma}$) only appear at later times. After reaching the lower surface of the slab, the shock wave propagation becomes similar to that in 2D systems.

Concerning the role of the different collective excitation modes in the screening, at $t \leq 150$ a.u. we observe ultrafast charge waves propagating along the slab surfaces due to excitation of the surface plasmon modes. At $t \geq 200$ a.u. it is also possible to resolve at the surface the soliton-like charge waves corresponding to the excitation of an acoustic surface plasmon. They propagate along the surface with velocity close to the group velocity of the acoustic surface plasmon. The formation of this soliton-like charge wave is related to the quasi-linear dispersion of the ASP mode.

The screening of charged particles in electronic media is therefore a local phenomenon in the subfemtosecond time scale, but collective excitations help to transfer electronic oscillations of charge to larger distances at longer time scales.

Spin-Selective Ultrafast Transfer of Electrons

Electron dynamics in the femtosecond scale are commonly analyzed by means of laser pump-probe techniques. Going beyond this ultrafast regime, under the same experimental scenario, would require attosecond laser pulses. Although attosecond pulses have been fully characterized, they must be composed of short wavelengths and can only be realized in the extreme ultraviolet and X-ray regimes (35). In order to monitor the dynamics of electron transfer at other frequencies in the attosecond time scale, alternative experimental approaches have been proposed. Core-hole spectroscopy has proven to be a successful one (36). Core-hole clock spectroscopy is based on using the core-hole lifetime of an adsorbate as an internal reference clock. The temporal evolution of the electronic process under scrutiny is then monitored in this new time frame (37).

Using CosterKronig autoionization processes as reference timescale, Föhlisch et al. measured elastic charge transfer times between adsorbed excited S atoms and Ru(0001) surfaces as fast as 320as (36). Density functional theory (DFT) calculations, together with a recursive method to obtain the Green's function of the surface, showed to be a remarkably reliable method to analyze such processes (38, 39). They predicted a peculiar dependence of the charge transfer times on the exciting light polarization that was experimentally confirmed (40). Besides the S/Ru (0001) system, Ar monolayers on Ru(0001) also have been theoretically studied (38), finding again values and trends for the charge-transfer times in good agreement with core-hole-clock experiments. This methodology was also used to calculate the elastic contribution to the total widths of quantum well states in alkali overlayers on Cu(111) (41), explaining the scanning tunneling spectroscopy (STS) spectra of such surfaces.

Here we use the same methodology to calculate the ultrafast charge transfer times between Cs atoms adsorbed at low coverage and the ferromagnetic Fe(110) surface. We consider that a localized hole is formed in the spin-orbit-split 5*p* level, and the excited electron is assumed to be well represented by the bound 6*s* resonance of the adsorbed Cs. Experimentally, photoexcitation with circularly polarized light permits such spin-selective excitation (42). We show that, as a consequence of the difference in the Fe(110) surface band structure between electrons with opposite spin orientations, the charge transfer is strongly spin-dependent. Due to the highest density of unoccupied *d* states with minority spin in the Fe(110) surface at the resonance energy position, one may naively think that the elastic electron transfer from the excited Cs 6*s* resonance to the surface would be much faster for excited electrons with this spin orientation. However, this is not the case: Surprisingly, charge transfer times are lower for majority-spin excitations.

Extensive details on the theoretical basis and on the computational scheme can be found in ref. 39 and are only summarized here. The first step is the DFT calculation of a finite slab. Slab calculations are performed using a linear combination of localized atomic orbitals as a basis set with the SIESTA code (43, 44). This information is then combined with that obtained from a bulk calculation of the substrate material. The Hamiltonian of the semiinfinite system is then built. The transfer-matrix method is used to compute the semiinfinite system Green's function.

In our particular case, the Fe slab contains seven metal layers plus a Cs atom adsorbed both on the upper and bottom surfaces. We use a (4×4) supercell to represent the surface, which is equivalent to consider a Cs coverage of 1/16 monolayers. The energy position and width of the Cs 6*s* resonance are theoretically obtained from the optimized projection of the Green's function on a wavepacket localized at the adsorbate (39). We have checked that this position is barely dependent on whether we consider the resonance as unoccupied or we perform a constrained calculation, with the resonance populated and a core hole in the Cs 5 p level. In both cases the resonance position is always between 2 and 2.5 eV above the Fermi level, and the difference between the position of the majority and minority spin resonances is always quite small.

Fig. 3 shows the calculated band structure of the Fe(110) surface for both spin orientations. The calculated position of the unoccupied Cs 6*s* resonance is shown as well. Side panels show the density of states (DOS) projected on the Fe surface atoms. Different symmetries for the electronic states are shown

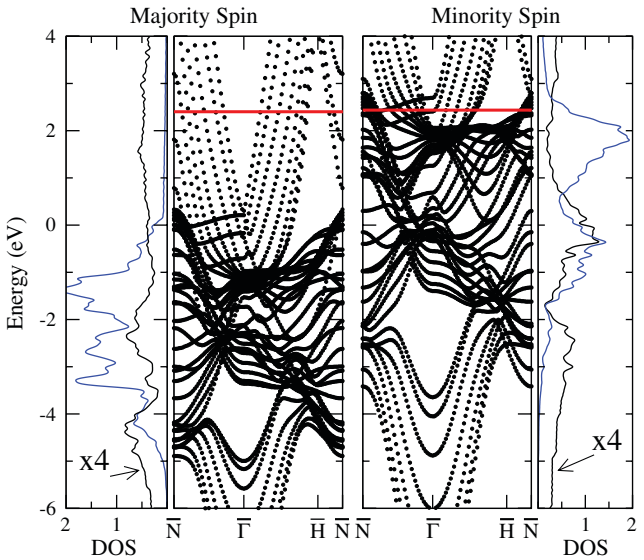

Fig. 3. Calculated band structure of the Fe(110) surface. Left (right) panel shows the majority (minority) spin results. The red straight line shows the energy position of the Cs resonance. Energies (in eV) are referred to the Fermi energy. The density of states (DOS) projected on a Fe surface atom is shown as well. Blue (black) lines show the contribution of 3*d* (4*sp*) orbitals. The 4*sp* DOS is multiplied by a factor of 4 for the sake of clarity.

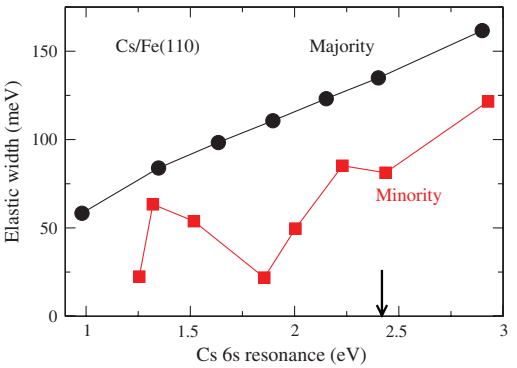

Fig. 4. Calculated elastic width of the Cs 6*s*-resonance in Fe(110) (in meV) as a function of the resonance energy position (in eV). The small black arrow shows the calculated position of the resonance. Black circles (red squares) show the results for an excitation with spin orientation parallel to that in the majority (minority) band of Fe(110). Lines are drawn to guide the eye. Energies (in eV) are referred to the Fermi energy.

separately. The minority-spin DOS has a clear peak at 2 eV above the Fermi level, due to the *d* bands of Fe. This peak partially overlaps with the Cs 6*s* resonance. Above the Fermi level, the 4*sp* DOS shows a similarly flat behavior for both spin orientations, although the absolute value near the Cs 6*s* resonance is slightly higher for majority spin.

An accurate estimate of the resonance width would require an integral over the bidimensional BZ of the supercell. In the following, however, we focus on the results calculated at the $\bar{\Gamma}$ point of our (4×4) supercell, which, according to our calculations, are representative of the global behavior. Using $\bar{\Gamma}$ in our supercell is equivalent to covering 16 **k** points in the surface BZ of the original Fe(110) unit cell. Despite the higher 3*d* DOS for the minority-spin channel at the Cs resonance energy, our calculations show that the width of the 6*s* resonance for majority spin is actually 135 meV, while the width for minority spin is only 81 meV. In other words and counterintuitively, the elastic transfer time for majority-spin excited electrons is appreciably shorter than that of electrons with minority spin.

A possible reason for that might have been an inefficient coupling of the Cs 6*s*-resonance with the Fe 3*d* states, due to the energy position of the resonance. The calculated resonance energy appears just at the tail of the 3*d* peak in the minority DOS. However, due to the use of DFT, inaccuracies in the position of the excited states can be expected. For this reason, we repeat the calculations progressively shifting down the Cs resonance (39) so that the Cs-3*d*Fe coupling could be favored. We show in Fig. 4 the calculated elastic width of the Cs 6*s* resonance in Fe(110) for majority and minority spin orientations as a function of the resonance energy position. The majority spin width keeps being higher than the minority one for the full range of energies considered. As it crosses the minority 3*d* band, the minority Cs resonance develops certain asymmetry. The fitting to a Lorentzian function in order to extract the width becomes more involved in this case. For this reason, a nonmonotonous behavior in the calculated width as a function of the resonance energy is found, but the overall trend is still robust.

Fig. 4 reinforces our previous claim that, surprisingly, elastic electronic transfer from the excited Cs adsorbate to the Fe(110) surface is faster for electrons with spin orientation parallel to the majority band in Fe bulk. This is so even if the available unoccupied DOS at the surface is largely of minority character. The ultimate reason for that is a stronger coupling of the 6*s* resonance to the *sp* states of the Fe surface, as compared to the coupling to the *d* states, due to orbital spacial extension. We stress that the *sp* DOS is roughly 50% higher for majority spin than for minority spin at the resonance energy position. Magnetization of unoccupied states at the Fe(110) surface is known to vary the sign when moving away from the Fe surface layer to the vacuum (47), and these exponentially decaying wave functions are the ones driving the elastic transfer. Therefore, elastic transfer of electrons from excited alkali atoms to a ferromagnetic surface can be spin-selective in a controlled way, with width values depending on spin orientation. However, whether the charge transfer is faster for majority-spin or for minority-spin electrons will be system-dependent and determined by the particular coupling conditions between the resonance and the surface band structure.

Confinement Effects in Electron Dynamics

Aside from spin effects, confinement in a given direction of space can provide a different degree of freedom for the tuning of the lifetimes of electronic excited states (45, 46). In quantum well states (QWS) formed in overlayers of Na over Cu(111), for instance, the amount of alkali atom coverage on the metal surface leads to a shift of the QWS energy band. As a consequence of the shift, an appreciable change in the linewidth is found leading to an appreciable size-dependent lifetime (48). This conclusion, however, does not apply to other systems in the nanoscale. Recent calculations of electron lifetimes in metal nanoparticles showed that, for particle sizes up to a few nanometers, the lifetime does not depend much on size (49, 50). Still, the lifetime value is surprisingly different from the bulk limit. This fact can be explained in terms of the partial localization of the electron excitation in the vicinity of the surface (50).

Quasiparticle lifetimes in ultrathin metal films are not well understood, in part because of the complex electronic structure at the substrate-overlayer interface. Surface states and quantum-well-type states can hybridize and drastically change the electronic properties at the interface (51). Additional complication is created by electronic transport that results in shorter experimental lifetimes compared to those expected theoretically (52, 53).

Recently, a model overlayer system, namely Pb(111) overlayers on Si(111) and Cu(111), was studied by scanning tunneling (54) and two-phototon photoemission (55) techniques. Theoretical calculations have also addressed these systems (54, 56). Experimentally, it was shown that the lowest electron excited state energy oscillates with the Pb film thickness, leading to strong oscillations in the electron–electron (*e*-*e*) (55) and elec-

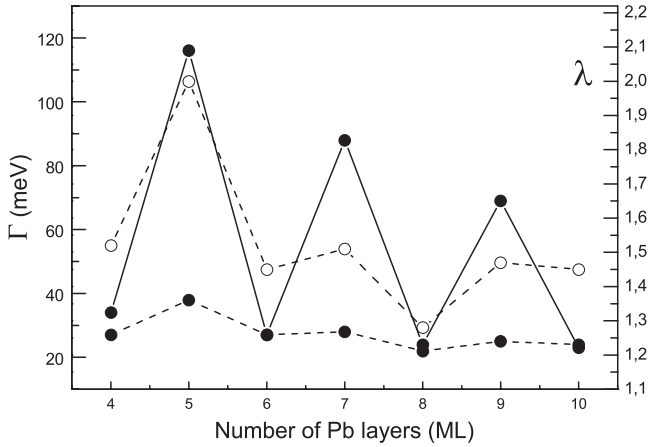

Fig. 5. Many-body $e-e$ (solid circles connected by solid line) and $e-ph$ (solid circles connected by dashed line) contribution to the lifetime broadening of the lowest unoccupied quantum-well state in Pb(111) free standing ultrathin films. $E-ph$ coupling parameter λ in these states is also shown (open circles connected by dashed line).

tron–phonon (e-ph) (54) scattering contributions to the lifetime broadening.

We present in Fig. 5 ab initio theoretical results for $\Gamma_{e\text{-}e}$, $\Gamma_{e\text{-}ph}$, and electron–phonon coupling strength parameter λ for the lowest unoccupied state of free standing relaxed ultrathin Pb(111) films in the range of 3 to 10 atomic monolayers.

As follows from the figure, all these quantities oscillate in phase with each other. Indeed, in good agreement with experimental findings, it can be shown that they oscillate in phase with the energy position of the lowest unoccupied QWS, as determined from calculations and time-resolved two-photon photoemission measurements (55). The behavior of both $\Gamma_{e\text{-}e}$ and $\Gamma_{e\text{-}ph}$ as a function of the film thickness shows that it is possible to tailor the lifetime of electronic excitations by means of thin-film nanofabrication.

Another remarkable feature of the Pb overlayer systems is the Fermi-liquid behavior of the excited electrons starting from a single Pb monolayer (54, 55). This is corroborated by relativistic calculations of the e-e contribution for bulk Pb, especially for the parent band of the Pb(111) QWSs, the bulk band which crosses E_F along the ΓL direction. Even the inclusion of the e-ph contribution to the lifetime broadening of excited states at relatively low temperatures does not deviate the lifetime broadening from the quadratic dependence on energy (54). This dependence can be explained by strong screening effects in Pb systems. The Thomas–Fermi screening length λ_s for bulk Pb is equal to 0.52 Å, which is significantly shorter than the Pb(111) interlayer spacing $d = 2.86$ Å. This means that the e-e interaction is screened in a way similar to that in bulk already in films of 1–2 ML thickness and explains why one can expect the energy dependence of the lifetime in Pb films to be similar to that in Pb bulk.

Conclusions and Future Directions

In summary, we have presented new results that illustrate some research lines currently active in the general field of time-dependent electron phenomena at metal surfaces. First, we have shown that the screening of localized charges at surfaces is created locally in the attosecond time scale, while collective excitations are able to transfer the perturbation to larger distances in longer time scales. We have predicted that the elastic width of the resonance in excited alkali adsorbates on ferromagnetic surfaces depends on spin orientation. Surprisingly, and due to a more efficient coupling, electrons with majority-spin orientation are faster than those with minority spin in Cs/Fe(110), even if the unoccupied DOS at the resonance energy position is higher for the latter. Finally, we have demonstrated that confinement effects can be used to control the timing of electronic decay at surfaces: The most important channels contributing to the electron lifetimes in ultrathin Pb films oscillate in phase as a function of the thickness in metal ultrathin films, in agreement with experimental measurements.

In addition, there are other topics within the general field of electron dynamics at surfaces in which intense activity is envisioned in the years to come. Among them, let us start by quoting the effects of adsorbates on acoustic surface plasmons (31). Adsorbed species at surfaces can shift the energy of surface states and modify their position relative to the Fermi level. In this way, the excitation channel linked to the acoustic surface plasmon can be switched on (or off), much affecting electron dynamics and the chemical properties of the surface.

In our results, we have focused on metal surfaces, but work on buried interfaces (57) and semiconductor surfaces (58–60) is equally important. Concerning C-based materials, superatom states of adsorbed fullerenes can lead to the formation of free electron bands (61). Endohedral doping of fullerenes offers then a route to tailor the superatom state properties. Actually, the functionalization of surfaces with molecules and clusters is a rapidly growing field. The switching properties of adsorbed molecules and their capabilities to create interface-specific electronic states are being extensively explored to control charge carrier transport (64).

Promising perspectives have been opened by the application of attosecond streaking techniques to solid surfaces (14). Attosecond spectroscopy could directly observe charge transfer between adsorbates and surfaces or between different species in chemical reactions. Progress in many aspects of surface chemistry currently demands experimental tools capable of simultaneous spatial and temporal resolution when studying dynamical phenomena in the nanometer scale. Interferometric time-resolved photoemission electron microscopy (ITR-PEEM), for instance, is able to explore quantum coherent phenomena on the attosecond time scale (62). Although primarily employed to image plasmonic phenomena at metal-vacuum interfaces (63), ITR-PEEM should in principle be able to achieve nanometer resolution beyond the ultrafast scale.

Finally, the interest on spin-dependent electron dynamics is based on its connection to practical applications in spintronics. The success of future devices relying on the electron spin as information carrier depends, among other things, on the possibility of transporting effectively a given spin state within a system. Promising materials to fulfill this goal are topological insulators (65, 66). These materials are characterized by topologically protected surface states that are spin-split due to strong spin-orbit interaction, thus carrying only one electron per momentum (67). Due to spin and linear momentum dependence (Dirac cone) of the surface states, these materials are of particular interest for electron and spin dynamics in molecules with magnetic atoms on the surface. Electron dynamics in these systems should be determined by the strong interplay between charge, spin, and vibrational degrees of freedom.

ACKNOWLEDGMENTS. We acknowledge partial support by the Basque government, the University of the Basque Country UPV/EHU (Grant No. 9/UPV 00206.215-13639/2001), and the Spanish Ministerio de Educación y Ciencia (Grant FIS2007-66711-C02-00).

1. Schmuttenmaer CA, et al. (1994) Time resolved two photon photoemission from Cu (100): Energy dependence of electron relaxation. *Phys Rev B* 50:8957–8960.
2. Höfer U, et al. (1997) Time-resolved coherent photoelectron spectroscopy of quantized electronic states on metal surfaces. *Science* 277:1480–1482.
3. Kliewer J, et al. (2000) Dimensionality effects in the lifetime of surface states. *Science* 288:1399–1402.
4. Weinelt M (2002) Time-resolved two-photon photoemission from metal surfaces. *J Phys-Condens Mat* 14:R1099–R1141.

5. Echenique PM, et al. (2004) Decay of electronic excitations at metal surfaces. *Surf Sci Rep* 52:219–317.
6. Güdde J, Rohleder M, Meier T, Koch SW, Höfer U (2007) Time-resolved investigation of coherently controlled electric currents at a metal surface. *Science* 318:1287–1291.
7. Osma J, Sarria I, Chulkov EV, Pitarke JM, Echenique PM (1999) Role of the intrinsic surface state in the decay of image states at a metal surface. *Phys Rev B* 59:10591–10598.
8. Lei J, Sun H, Yu KW, Louie SG, Cohen ML (2001) Image potential states on periodically corrugated metal surfaces. *Phys Rev B* 63:045408.
9. Lopez-Bastidas C, Maytorena JA, Liebsch A (2001) Hot-electron dynamics at noble metal surfaces. *Phys Rev B* 65:035417.
10. Sakaue M, Munakata T, Kasai H, Okiji A (2003) Effects of hole scattering on two-photon photoemission from metal surfaces. *Phys Rev B* 68:205421.
11. Chulkov EV, et al. (2006) Electronic excitations in metal and at metal surfaces. *Chem Rev* 106:4160–4206.
12. Schone WD (2007) Theoretical determination of electronic lifetimes in metals. *Prog Surf Sci* 82:161–192.
13. Ueba H, Gumhalter B (2007) Theory of two-photon photoemission spectroscopy of surfaces. *Prog Surf Sci* 82:193–223.
14. Cavalieri AL, et al. (2007) Attosecond spectroscopy in condensed matter. *Nature* 449:1029–1032.
15. Kazansky AK, Echenique PM (2009) One-electron model for the electronic response of metal surfaces to subfemtosecond photoexcitation. *Phys Rev Lett* 102:177401–1-4.
16. Aeschlimann M, et al. (1997) Ultrafast spin-dependent electron dynamics in fcc Co. *Phys Rev Lett* 79:5158–5161.
17. Bauer M, Pawlik S, Aeschlimann M (1997) The resonance lifetime and energy of an excited Cs-state on Cu(111). *Phys Rev B* 55:10040–10043.
18. Ogawa S, Nagano H, Petek H (1999) Phase and energy relaxation in an antibonding surface state: Cs/Cu(111). *Phys Rev Lett* 82:1931–1934.
19. Petek H, Weida MJ, Nagano H, Ogawa S (2000) Real-time observation of adsorbate atom motion above a metal surface. *Science* 288:1402–1404.
20. Borisov AG, Gauyacq JP, Chulkov EV, Silkin VM, Echenique PM (2002) Lifetime of excited electronic states at surfaces: Comparison between the alkali/Cu(111) systems. *Phys Rev B* 65:235434–1-10.
21. Borisov AG, et al. (2008) π-resonance of chemisorbed alkali atoms on noble metals. *Phys Rev Lett* 101:266801–1-4.
22. Zhao J, et al. (2008) Electronic potential of a chemisorption interface. *Phys Rev B* 78:085419–1-7.
23. Huber R, et al. (2001) How many-particle interactions develop after ultrafast excitation of an electron-hole plasma. *Nature* 414:286–289.
24. Haug H, Jauho AP (1998) *Quantum Kinetics in Transport and Optics of Semiconductors* (Springer-Verlag, Berlin).
25. Canright GS (1988) Time-dependent screening in the electron gas. *Phys Rev B* 38:1647–1653.
26. Borisov A, Sánchez-Portal D, Díez Muiño R, Echenique PM (2004) Building up the screening below the femtosecond scale. *Chem Phys Lett* 387:95–100.
27. Alducin M, Juaristi JI, Echenique PM (2004) Time-dependent screening in a two-dimensional electron gas. *Surf Sci* 559:233–240.
28. Borisov A, Sánchez-Portal D, Díez Muiño R, Echenique PM (2004) Dimensionality effects in time-dependent screening. *Chem Phys Lett* 393:132–137.
29. Lazić P, Silkin VM, Chulkov EV, Echenique PM, Gumhalter B (2006) Extreme ultrafast dynamics of quasiparticles excited in surface electronic bands. *Phys Rev Lett* 97:086801–1-4.
30. Silkin VM, et al. (2004) Novel low-energy collective excitations at metal surfaces. *Europhys Lett* 66:260–264.
31. Diaconescu B, et al. (2007) Low-energy acoustic plasmons at metal surfaces. *Nature* 448:57–59.
32. Chulkov EV, Silkin VM, Echenique PM (1999) Image potential states on metal surfaces: Binding energies and wave functions. *Surf Sci* 437:330–352.
33. Ritchie RH (1957) Plasma losses by fast electrons in thin films. *Phys Rev* 106:874–881.
34. Silkin VM, Alducin M, Juaristi JI, Chulkov EV, Echenique PM (2008) The role of an electronic surface state in the stopping power of a swift charged particle in front of a metal. *J Phys-Condens Mat* 20:304209–1-7.
35. Cavalieri A (2010) Beyond ultrafast. *Phys Today* 23(5):47–51.
36. Föhlisch A, et al. (2005) Direct observation of electron dynamics in the attosecond domain. *Nature* 436:373–376.
37. Wurth W, Menzel D (2000) Ultrafast electron dynamics at surfaces probed by resonant Auger spectroscopy. *Chem Phys* 251:141–149.
38. Sánchez-Portal D, Menzel D, Echenique PM (2007) First principles calculation of charge transfer at surfaces: The case of core-excited $Ar^*(2p_{-1}^{3/2}4\,s)$ on Ru, (0001). *Phys Rev B* 76:235406–1-19.
39. Sánchez-Portal D (2007) Slab calculations and Greens function recursive methods combined to study the electronic structure of surfaces: Application to Cu(111)(4×4)-Na. *Prog Surf Sci* 82:313–335.
40. Deppe M, et al. (2007) Ultrafast charge transfer and atomic orbital polarization. *J Chem Phys* 127:174708–1-5.
41. Corriol C, et al. (2005) Role of elastic scattering in electron dynamics at ordered alkali overlayers on Cu(111). *Phys Rev Lett* 95:176802–1-4.
42. Schönhense G, Eyers A, Heinzmann U (1986) Sharp photon-induced np $\rightarrow (n+1)$s resonances in Xe and Kr monolayers observed by spin-resolved electron spectroscopy. *Phys Rev Lett* 56:512–515.
43. Sánchez-Portal D, Ordejón P, Artacho E, Soler JM (1997) Density-functional method for very large systems with LCAO basis sets. *Int J Quantum Chem* 65:453–461.
44. Soler JM, et al. (2002) The SIESTA method for ab initio order-N materials simulation. *J Phys-Condens Mat* 14:2745–2779.
45. Wu R, Freeman AJ (1992) Spin density at the Fermi level for magnetic surfaces and overlayers. *Phys Rev Lett* 69:2867–2870.
46. Mathias S, et al. (2010) Band structure dependence of hot-electron lifetimes in a Pb/Cu (111) quantum-well system. *Phys Rev B* 81:155429–1-8.
47. Mathias S, et al. (2010) Quantum-well-induced giant spin-orbit splitting. *Phys Rev Lett* 104:066802–1-4.
48. Silkin VM, Quijada M, Díez Muiño R, Chulkov EV, Echenique PM (2007) Dynamic screening and electron-electron scattering in low-dimensional metallic systems. *Surf Sci* 601:4546–4552.
49. Quijada M, Díez Muiño R, Echenique PM (2005) The lifetime of electronic excitations in metal clusters. *Nanotechnology* 16:S176–S180.
50. Quijada M, Díez Muiño R, Borisov AG, Alonso JA, Echenique PM (2010) Lifetime of electronic excitations in metal nanoparticles. *New J Phys* 12:053023–1-9.
51. Hirahara T, et al. (2006) Role of spin-orbit coupling and hybridization effects in the electronic structure of ultrathin Bi films. *Phys Rev Lett* 97:146803–1-4.
52. Ogawa S, Nagano H, Petek H (2002) Optical intersubband transitions and femtosecond dynamics in Ag/Fe(100) quantum wells. *Phys Rev Lett* 88:116801–1-4.
53. Zhukov VP, et al. (2007) Excited electron dynamics in bulk Ytterbium: time-resolved two-photon photoemission and GW + T ab initio calculations. *Phys Rev B* 76:193107–1-4.
54. Hong IP, et al. (2009) Decay mechanisms of excited electrons in quantum-well states of ultrathin Pb islands grown on Si(111): Scanning tunneling spectroscopy and theory. *Phys Rev B* 80:081409(R)–1-4.
55. Kirchmann PS, Bovensiepen U (2008) Ultrafast electron dynamics in Pb/Si(111) investigated by two-photon photoemission. *Phys Rev B* 78:035437–1-7.
56. Zugarramurdi A, Zabala N, Silkin VM, Borisov AG, Chulkov EV (2009) Lifetimes of quantum well states and resonances in Pb overlayers on Cu(111). *Phys Rev B* 80:115425–1-11.
57. Rohleder M, Berthold W, Güdde J, Höfer U (2005) Time-resolved two-photon photoemission of buried interface states in Ar/Cu(100). *Phys Rev Lett* 94:017401–1-4.
58. Weinelt M, Kutschera M, Fauster Th, Rohlfing M (2004) Dynamics of exciton formation at the Si(100) $c(4\times2)$ surface. *Phys Rev Lett* 92:126801–1-4.
59. Voelkmann C, Reichelt M, Meier T, Koch SW, Höfer U (2004) Five-wave-mixing spectroscopy of ultrafast electron dynamics at a Si(001) surface. *Phys Rev Lett* 92:127405–1-4.
60. Rügheimer TK, Fauster Th, Himpsel FJ (2007) Unoccupied electronic states in atomic chains on Si(557)-Au: Time-resolved two-photon photoemission investigation. *Phys Rev B* 75:121401–1-4.
61. Feng M, Zhao J, Petek H (2008) Atomlike, hollow-corebound molecular orbitals of C_{60}. *Science* 320:359–362.
62. Schwalb CH, et al. (2008) Electron lifetime in a Shockley-type metal-organic interface state. *Phys Rev Lett* 101:146801–1-4.
63. Kubo A, et al. (2005) Femtosecond imaging of surface plasmon dynamics in a nanostructured silver film. *Nano Lett* 5:1123–1127.
64. Kubo A, Pontius N, Petek H (2007) Femtosecond microscopy of surface plasmon polariton wave packet evolution at the silver/vacuum interface. *Nano Lett* 7:470–475.
65. Kane CL (2008) Condensed matter: An insulator with a twist. *Nat Phys* 4:348–349.
66. Moore JE (2009) Topological insulators: The next generation. *Nat Phys* 5:378–380.
67. Eremeev SV, Koroteev YM, Chulkov EV (2010) Effect of the atomic composition of the surface on the electron surface states in topological insulators $A_2^{\rm V}B_3^{\rm VI}$. *JETP Lett* 91:387–391.